

# TIME-SLICED EMITTANCE AND ENERGY SPREAD MEASUREMENTS AT FERMI@ELETTRA\*

G. Penco<sup>†</sup>, E. Allaria, P. Craievich<sup>‡</sup>, G. De Ninno, S. Di Mitri, W. B. Fawley, E. Ferrari,  
L. Giannessi, C. Spezzani, M. Trovò, Sincrotrone Trieste, Italy  
S. Spampinati, SLAC, Menlo Park, California, USA

## Abstract

FERMI@Elettra is a single pass seeded FEL based on the high gain harmonic generation scheme, producing intense photon pulses at short wavelengths. For that, a high-brightness electron beam is required, with a small uncorrelated energy spread. In this paper, we present a detailed campaign of measurements aimed at characterizing the electron-beam time-sliced emittance and energy spread, both after the first magnetic compressor and at the end of the linac.

## INTRODUCTION

The FERMI@Elettra free electron laser (FEL) at the Elettra Laboratory of Sincrotrone Trieste [1] is a major European FEL project. FERMI is a single-pass, S-band linac-based externally seeded FEL implementing high gain harmonic generation in the 80-4 nm fundamental output wavelength range [2]. The commissioning of the first stage, named FEL-1, has been completed, providing intense photon beams (few hundreds of micro Joules) ranging from 80nm to 20nm [3] to the beam-lines for first preliminary experiments. A high brightness electron beam with small energy spread was required to guarantee the high quality performance of the FEL and a strong effort was spent to preserve the beam transverse emittance after the longitudinal compression. Nevertheless, the transverse emittance and the uncorrelated energy spread may strongly vary along the bunch due to collective effects, as space-charge forces and coherent synchrotron radiation, which have an important role especially when the charge density increased during the longitudinal compression. Since only a fraction of the electron bunch is interested in the interaction with the seed laser to carry on the FEL process, it is crucial to measure and to control the time-sliced emittance and energy spread. The layout of the FERMI linac includes two magnetic chicanes to longitudinally compress the electron bunch, located respectively at about 320MeV and at about 670MeV. Two RF deflecting cavities were installed respectively after the first magnetic chicane (low energy RF deflector, LERFD) and at the end of the linac (high energy RF deflector, HERFD), to measure the horizontal time-sliced emittance and, by sending the electrons in the close spectrometer, to measure the time-sliced energy spread. A third RF deflecting cavity is going to be installed at the end of

the linac to horizontally "stretch" the beam and investigate the vertical time-sliced emittance.

## TIME SLICED EMITTANCE

The design goal illustrated in the CDR [4] is sending into the undulators beam-lines a 750A-600fs (full width in the core) electron bunch with a slice emittance below 1.5  $\mu\text{m}$ . At the present, the FERMI photoinjector has been providing a 500pC bunch, 2.8 ps long (rms) which is longitudinal compressed by about a factor 10 in the first bunch compressor. As already mentioned, the low energy RF deflecting cavity (LERFD) is located just after the first magnetic chicane (BC1), allowing measuring the slice parameters of the beam after the longitudinal compression [5]. The LERFD cavity is a five cell standing wave structure, sharing the same klystron of the electron gun. An attenuator and a phase shifter allow to independently modulate the input power. The required deflecting voltage  $V_t = 3\text{MV}$  can be reached with an input power  $P_{in} = 1.9\text{MW}$  and a maximum electric peak of  $E_p = 48\text{MV/m}$ . After the LERFD cavity, four quadrupoles and three multi-screens stations are placed for measuring the beam optics parameters and matching them after the longitudinal compression (see the layout in figure 1).

The Twiss function and the emittance measurements have been performed by implementing the well known quadrupole scan technique [6], by using the fourth quadrupole and the second screen, placed in correspondence of the beam waist, at about 9 meters from the LERFD cavity. The multi-screen stations are equipped with Optical Transition Radiation (OTR) and Yttrium Aluminum Garnet (YAG) targets. For improving the emittance measurement accuracy we have used the OTR targets, that could provide a beam spot size estimation with 20 $\mu\text{m}$  resolution. Nevertheless for high compression factor, the OTR targets suffer from coherent optical transition radiation that corrupts the beam spot image. This effect has been mitigated by the implementation of the X-band cavity that linearizes the longitudinal phase space and flats the beam current profile, and by the activation of the Laser Heater [7]. Figure 2 shows the comparison between the OTR image of the same beam spot (a compressed beam ( $\sigma_t \approx 1\text{ps}$  at 300MeV) with and without the laser heater working. The signal intensity drops sensitively when activating the laser heater and this indicates that microbunching structures along the bunch are present already at moderate compression factor. Thus in order to have a reliable measurement of the beam spot size with OTR screens, it is necessary to switch on the

\* This work was supported in part by the Italian Ministry of University and Research under grants FIRB-RBAP045JF2 and FIRB-RBAP-6AWK3

<sup>†</sup> giuseppe.penco@elettra.trieste.it

<sup>‡</sup> now working at Paul Scherrer Institute

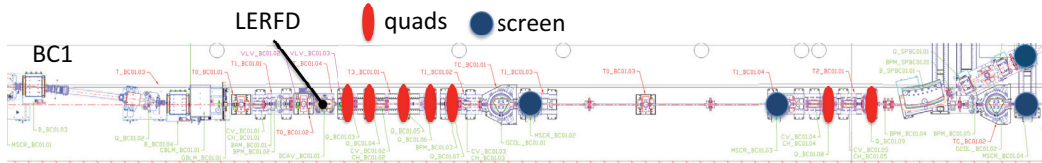


Figure 1: BC1 diagnostics layout.

laser heater. In the case of figure 2, the rms bunch length that we measured activating the laser heater is reduced from about  $160 \mu\text{m}$  to about  $100 \mu\text{m}$ .

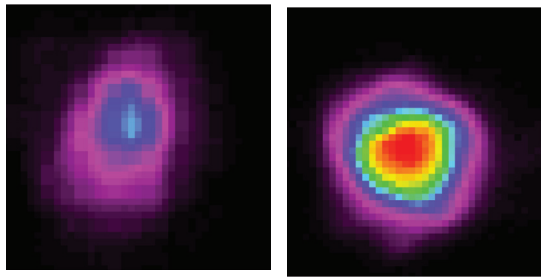


Figure 2: Beam spot on the 300MeV OTR target with Laser Heater in On (on the left) and in OFF (on the right). The CCD gain is kept constant. Pixel dimension =  $20 \mu\text{m}$ .

After performing the optics matching, the beam is vertically stretched by powering the RF deflecting cavity and figure 3 shows the typical beam spot acquired on the second OTR target. When the deflecting cavity is switched off, the beam spot dimension at this screen is about  $100 \mu\text{m}$  (rms), so the perturbation of the finite transverse emittance could be neglected, allowing to slice the streaked beam trace in several portions. The measured horizontal emittance of ten time-slices are plotted on the right of figure 3 for a 500pC-350fs long (rms) electron bunch. In this configuration all slices meet the specified target of  $1.5 \mu\text{m}$  emittance.

As anticipated in the Introduction, a second deflector (HERFD) was installed at the end of the linac to characterize the electron beam just before the FEL process in terms of slice emittance, slice energy spread and bunch length. We have preliminarily studied the double compression scheme, which resulted to be more critical in terms of reliability and reproducibility of the FEL performance. For this reason we focused on the single compression scheme to provide a reliable FEL for Users operations, planning to deeply investigate the two stages compression in the next future.

Therefore the HERFD measurements of the beam slice emittance provided results similar to what is obtained with

ISBN 978-3-95450-123-6

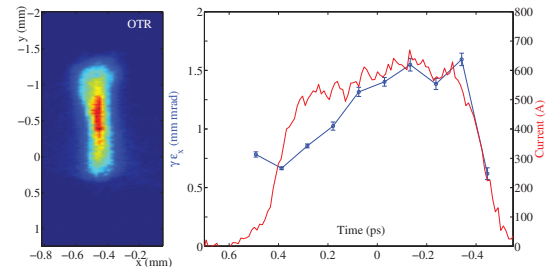


Figure 3: On the left: stretched beam spot acquired on the OTR target; on the right: current profile and slice emittance of a 500pC-370fs long bunch.

the LERFD cavity. Nevertheless, activating the HERFD and sending the beam in the close spectrometer at 1.2GeV has allowed investigating the longitudinal phase space of the electron bunch just before the undulators chains. Next section is dedicated to this subject.

## LONGITUDINAL PHASE SPACE MEASUREMENTS

Figure 4 shows the layout of the diagnostic area at the end of the FERMI linac, including the HERFD cavity, the third deflector that is to be installed next and the 1.2 GeV spectrometer beam-line, called Diagnostic Beam Dump (DBD). The HERFD cavity is a backward traveling wave structure, 2 meters long and working at 2.998GHz. We estimated a maximum deflecting voltage of 18.5MV, that satisfies the specified 18MV. For more details on the HERFD RF design optimization we refer to [8, 9].

When the electron bunch is simply propagated up to the end of the linac setting all the RF sections on crest, the longitudinal phase space presents the typical sinusoidal shape. In figure 5 we report the DBD screen image detected when HERFD is activated, rotating by 90 deg to help the readings. The vertical axis is converted in MeV according to the dipole dispersion ( $\eta = 1.74m$ ) and the horizontal axis in ps according to the HERFD calibration, executed scanning its RF phase around the zero crossing (corresponding to no deflection of the bunch centroid). The energy spread resolution is defined as:

$$\sigma_{E,res} = \frac{\sqrt{\epsilon\beta}}{\eta} E \quad (1)$$

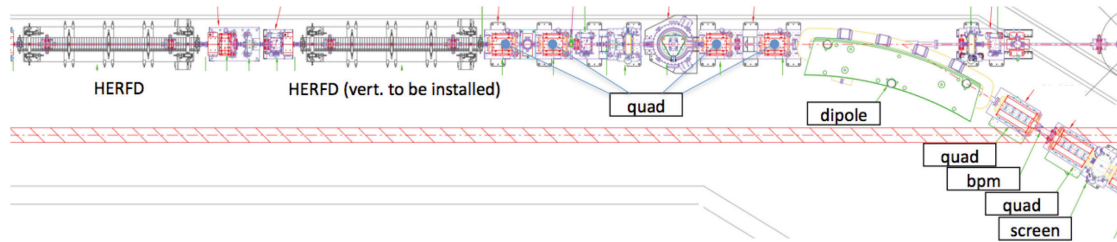


Figure 4: Beam diagnostic area at the FERMI linac end.

where  $\epsilon$  is the geometric emittance,  $\beta$  the betatron function at the screen and  $E$  the beam energy. For the nominal lattice we have  $\sigma_{E,res} = 40keV$ . Moreover we have to consider the screen system resolution of  $30 \mu m/pixel$ , corresponding approximately to the minimum rms beam size that can be measured at the screen. The screen resolution is comparable to the optical beam size in the DBD line, so adding the two contributions in quadrature we obtain a resolution of about  $\sigma_{E,res} = 60keV$ . Processing the acquired image we obtained the time-sliced behavior of the energy spread and of the current along the bunch. Results are plotted on the right of figure 5.

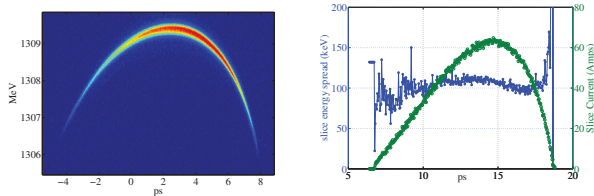


Figure 5: 500pC uncompressed bunch: longitudinal phase space (on the left) and slice energy spread and current profile (on the right).

The slice energy spread is around 100keV along the bunch. The longitudinal wakefields induced by a 500pC bunch when passing through linac sections upstream BC1 are not negligible and modify the energy distribution of the bunch itself. As a consequence, the current profile after BC1 is slightly asymmetric. When the bunch is shortened, the effects of the wakefields of the downstream linac becomes important and contribute in defining the final longitudinal phase space of the bunch. This latter is mainly affected by:

- RF curvature introduced by the linac upstream BC1, used for creating the linear chirp;
- RF curvature of the rest of the linac;
- first ( $R_{56}$ ) and second order ( $T_{566}$ ) terms of the magnetic chicane;
- RF curvature induced by the X-band, that linearizes the phase space before BC1;

- longitudinal wakefields in all RF sections;

High FEL performance in HGHG scheme requires low slice energy spread and a flat distribution of current and energy of electrons participating in the FEL process. In fact while a linear chirp in the bunch energy distribution mainly induces a frequency shift of the FEL radiation, a quadratic curvature enlarges the FEL radiation bandwidth [4]. In presence of a time jitter between the electron bunch and the seed laser of about 100fs (rms), the combination of linear and quadratic terms in the bunch energy distribution influences the spectrum and the intensity of the FEL radiation. Figure 6 shows the longitudinal phase space and the slice energy spread that we measured for several machine configurations. The first one refers to the single compression scheme (a factor 5) without X-band cavity and without laser heater, and setting on crest all RF sections downstream BC1. The bunch current profile presents a peak in the head of the bunch of about 400A (on the left in figure 6). The high charge density around this peak induces strong energy and current modulation (i.e. microbunching instabilities) that are visible as three “hot spots” in the plot on the left. In this portion of the bunch, the slice energy spread is large (about 300keV) and it deteriorates the FEL performance in terms of spectrum and intensity, especially at high harmonics [10].

In the second case we switched on the laser heater, suppressing the microbunching structures, but without X-band, the longitudinal compression is not linear and the current profile presents again a high peak in the head. We adjusted the seed laser time delay to make it overlaps the bunch portion just behind the high peak, which has a slice energy spread of about 200keV and a peak current around 200-250A. The seed laser bunch length is about 150fs (FWHM). Pushing further the compression enhances the head peak current but at the same time it increases also the slope of the current profile, squeezing the “good portion” of the electron bunch useful for the FEL process.

In the third case, X-band cavity is set on the decelerating crest, linearizing the longitudinal phase space before BC1 and flattening the current profile. This allows pushing the compression further, reaching peak current of 500-600A in a large portion of bunch. The residual slope in the current profile is due to a not optimized voltage and phase settings of the X-band cavity. In this condition, the bunch is very

short ( $\sigma_t = 300fs$ ) and the longitudinal wakefields have a strong influence on the final longitudinal phase space, introducing a linear and a quadratic chirp. The resulting longitudinal phase space has an opposite curvature relative to the uncompressed beam (see figure 5). The linear chirp might be compensated by changing the RF phase of some linac sections. Concerning the quadratic chirp, a possibility is changing the X-band phase by few degrees around the decelerating crest, but this affects the current profile flatness. The fourth case of figure 6 refers to the situation in which the X-band phase and voltage are optimized to obtain a flat current profile in the middle of the bunch. Furthermore the RF phase of the last two sections are set to +30deg (relative to the crest) to compensate the linear chirp. In this final configuration, a central portion of the bunch  $\approx 300fs$  long has a constant energy within 0.5MeV, a good slice energy spread (around 150-200keV) and a peak current greater than 600A. Operating the linac as the fourth case, the FEL flux is much more intense, but the residual quadratic chirp in the electron bunch however affects the FEL spectrum, broadening its bandwidth, but still satisfying Users requirements.

## CONCLUSION

The high FEL performance obtained in the FERMI machine is mainly due to the high brightness beam obtained at the end of the linac. By using the RF deflecting cavity just after the first bunch compressor, we measured a slice emittance of less than  $1.5 \mu m$  for a 500pC bunch, compressed about 10 times and having a peak current of about 600A. The high energy RF deflector installed at the end of the linac confirmed this result and in combination with the DBD spectrometer has allowed to characterize the longitudinal phase space with and without X-band cavity. Moreover it was very useful in the laser heater commissioning as shown in [7]. The linac optimization has included the tuning of the X-band RF parameters to flatten the current profile, the laser heater settings to suppress the microbunching instabilities and the RF phase of the last two accelerating sections to compensate the curvature induced by the longitudinal wakes. We measured for the resulting optimized electron bunch a slice energy spread of about 200keV, which allows to obtain FEL that meets specifications.

## REFERENCES

- [1] M.Svandrlík et al., TUOB03, Proc. of IPAC 2012 conference, New Orleans, Louisiana, USA (2012).
- [2] E. Allaria et al., "Highly coherent and stable pulses from the FERMI seeded free-electron laser in the extreme ultraviolet," to be published in Nature Photonics, 2012.
- [3] E. Allaria et al., TUPD01, Proc. of this Conference.
- [4] "Conceptual Design Report" for the FERMI@Elettra project (2007).
- [5] P. Craievich et al, WEPB43, Proc. of the FEL 2010 Conference, Malmö, Sweden (2010).

ISBN 978-3-95450-123-6

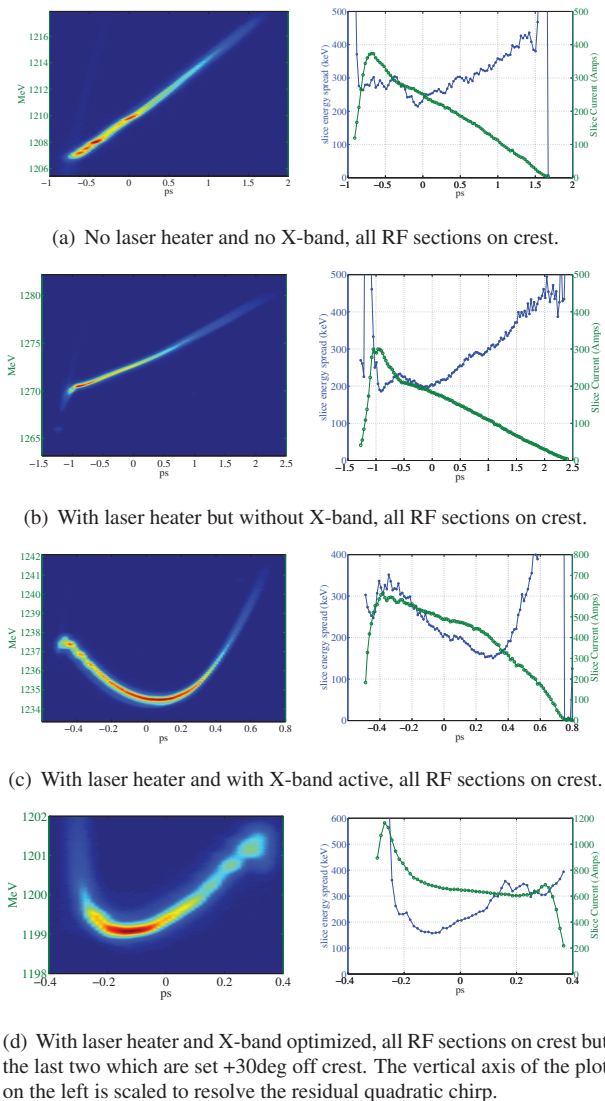


Figure 6: Longitudinal phase space of a 500pC bunch in different linac configurations.

- [6] G. Minty and F. Zimmermann, SLAC-R-621 (2003).
- [7] S.Spampinati et al., MOPD58, Proc. of this Conference.
- [8] P. Craievich et al., TUPC10, Proc. of the DIPAC 2007 Conference, Venice, Italy (2007).
- [9] M. Petronio, Thesis of degree, Università degli Studi di Trieste, April, 2007.
- [10] E. Allaria et al., TUOB02, Proc. of this conference.